Check for updates

Received: 2 June 2023 | Revised: 18 July 2023 | Accepted: 19 July 2023

DOI: 10.1002/ardp.202300302

FULL PAPER

ARCH PHARM DPhG
Archiv der Pharmazie

Design, synthesis, antimicrobial activity and molecular docking study of cationic bis-benzimidazole-silver(I) complexes

Elvan Üstün[1] | Neslihan Şahin[2] | İlknur Özdemir[3,4] | Selami Günal[5] | Nevin Gürbüz[3,4] | İsmail Özdemir[3,4] | David Sémeril[6]

[1]Department of Chemistry, Faculty of Art and Science, Ordu University, Ordu, Türkiye

[2]Department of Mathematics and Science Education, Cumhuriyet University, Sivas, Türkiye

[3]Department of Chemistry, Faculty of Science and Art, İnönü University, Malatya, Türkiye

[4]Drug Application and Research Center, İnönü University, Malatya, Türkiye

[5]Department of Microbiology, Faculty of Pharmacy, İnönü University, Malatya, Türkiye

[6]Synthèse Organométallique et Catalyse, UMR-CNRS 7177, University of Strasbourg, Strasbourg, France

Correspondence
David Sémeril, Synthèse Organométallique et Catalyse, UMR-CNRS 7177, University of Strasbourg, 4 rue Blaise Pascal, Strasbourg 67008, France.
Email: dsemeril@unsitra.fr

Neslihan Şahin, Department of Mathematics and Science Education, Faculty of Education, Cumhuriyet University, Yenisehir District, Sivas 58140, Türkiye.
Email: neslihan@cumhuriyet.edu.tr

Funding information
Scientific Research Project Fund of Sivas Cumhuriyet University

Abstract

Two series of bis(1-alkylbenzimidazole)silver(I) nitrate and bis(1-alkyl-5,6-dimethylbenzimidazole)silver(I) nitrate complexes, in which the alkyl substituent is either an allyl, a 2-methylallyl, an isopropyl or a 3-methyloxetan-3-yl-methyl chain, were synthesized and fully characterized. The eight *N*-coordinated silver(I) complexes were screened for both antimicrobial activities against Gram-negative (*Escherichia coli*, *Pseudomonas aeruginosa*, *Klebsiella pneumoniae*, and *Acinetobacter baumannii*) and Gram-positive (*Staphylococcus aureus*, *Staphylococcus aureus* MRSA, and *Enterococcus faecalis*) bacteria and antifungal activities against *Candida albicans* and *Candida glabrata* strains. Moderate minimal inhibitory concentrations (MIC) of 0.087 µmol/mL were found when the Gram-negative and Gram-positive bacteria were treated with the silver complexes. Nevertheless, MIC values of 0.011 µmol/mL, twice lower than for the well-known fluconazole, against the two fungi were measured. In addition, molecular docking was carried out with the structure of *Escherichia coli* DNA gyrase and CYP51 from the pathogen *Candida glabrata* with the eight organometallic complexes, and molecular reactivity descriptors were calculated with the density functional theory-based calculation methods.

KEYWORDS
antifungal activity, antimicrobial activity, benzimidazole, molecular docking, silver

1 | INTRODUCTION

Heterocyclic compounds, organic cyclic molecules generally composed of at least one nitrogen, oxygen, or sulfur atom, are an important family of organic compounds whose chemical and physical properties depend on the size, the number, and the nature of the heteroatom. Among heterocyclic compounds, aromatic derivatives are particularly present in a large number, about 85%, of biologically active compounds such as serotonin (neurotransmitter) or nicotine.[1] In particular, among the nitrogenous heterocyclic compounds, the benzimidazole moiety, a bicyclic hetero-aromatic molecule incorporating two nitrogen atoms, plays an increasing role. These derivatives

This is an open access article under the terms of the Creative Commons Attribution-NonCommercial-NoDerivs License, which permits use and distribution in any medium, provided the original work is properly cited, the use is non-commercial and no modifications or adaptations are made.
© 2023 The Authors. *Archiv der Pharmazie* published by Wiley-VCH GmbH on behalf of Deutsche Pharmazeutische Gesellschaft.

have wide potential applications such as antibacterial, antiviral, antiparasitic, anthelmintic, antitumor, anti-inflammatory, antioxidant, antiulcer, antihypertensive, anticoagulant, antidepressant, anticonvulsant, antihistaminic, antiasthmatic, and antidiabetic agents.[2–11]

Although the use of compounds with an aromatic ring derived from benzimidazole as a biological agent is quite old, the study of the antimicrobial properties of these compounds accelerated in the early 1990s. For example, the group of Opferkuch, *in vitro*, investigated the bactericidal activities of substituted benzimidazoles against *Helicobacter pylori*, which is responsible for gastric acid secretion.[12] In the following years, various compounds derived from benzimidazole were synthesized and they demonstrated strong activity against various bacteria;[13–15] currently several of these derivatives such as albendazole, as an anthelmintic and antiprotozoal agent, mebendazole, used against parasitic worm infestations, or tiabendazole, an antifungal and an antiparasitic agent, are commercially available drugs (Figure 1).

Although there are many antibacterial drugs currently available, microbial resistance to antibiotics comes a major problem. Therefore, the development of new drug candidates against antimicrobial resistance is a necessity and therefore of interest to researchers. Consequently, the benzimidazole platform is particularly interesting due to its nitrogen atom being able to coordinate with transition metals[16–19] and especially with silver[20,21] or as a precursor of *N*-heterocyclic carbenes, for example, for bis-silver complexes.[22,23]

In this context, we now report the synthesis of eight cationic silver(I) complexes, in which two benzimidazole entities were coordinated through their nitrogen atom to the metal, and their antimicrobial activities against Gram-negative, Gram-positive, and Fungi strains. To better understand the antimicrobial and antifungal mechanisms of these silver salts, molecular docking analysis, and global reactivity descriptors complete the present study.

2 | RESULTS AND DISCUSSION

2.1 | Chemistry

Two series of bis(1-alkyl-benzimidazole)silver(I) nitrate (**2a–d**) and bis (1-alkyl-5,6-dimethyl-benzimidazole)silver(I) nitrate (**2e–h**) in which the alkyl substituent is either an allyl, 2-methylallyl, isopropyl or 3-methyloxetan-3-yl)methyl chain, were synthesized in two steps starting from benzimidazole or 5,6-dimethyl-benzimidazole scaffold according Scheme 1. In the first step, the alkylation of benzimidazole or 5,6-dimethyl-benzimidazole using NaH and the adequate alkylated agent in tetrahydrofurane (THF) led to the *N*-alkylated benzimidazole derivatives **1a–h**.[24–28] Afterwards, the silver(I) complexes (**2a–h**) were obtained, in 77%–85% yield, by reaction of $AgNO_3$ with two equivalents of nitrogenated ligands **1a–h** in ethanol for 4 h at room temperature protected from light with an aluminum foil.

The eight white silver complexes **2a–h** were stable to air and moisture in solid and solution but sensitive to light. These complexes were further characterized by elemental analysis, fourier-transform infrared spectroscopy (FT-IR), and multi-nuclear magnetic resonance (NMR) spectroscopy (^{1}H and ^{13}C) (see Section 4 and Supporting Information Materials). The presence of two nitrogenated ligands (L = **1a–h**) was unambiguously deduced from their elemental analysis, which perfectly fitted with the formation of $[AgL_2]^+NO_3^-$ salts. Note that, the presence of a water molecule in the elemental analysis of compounds **2b**, **2c**, **2d**, and **2g**. The presence of water, coming from the solvent of the reaction, was also visible on the FT-IR spectra as a wide band around 3500–3400 cm^{-1}. The coordination of a water molecule with $[AgL_2]^+$ cation is common and forms a T-shaped arrangement ($[AgL_2(H_2O)]^+$) as described by single crystal X-ray crystallography.[29]

The FT-IR spectra also displayed two characteristic bands, the first one in the range 1316–1335 cm^{-1} assigned to NO_3^- anion and the second one in the range 1503–1515 cm^{-1} assigned to C=N vibration of the benzimidazole moieties. Note that the values of the C=N bands were redshifted from 9 to 41 cm^{-1} in regards to the aromatic precursors **1a–h**. NMR analysis carried out on the silver complexes **2a–h** revealed for each compound the presence, as expected, of singlets in the range 8.50–8.77, with a shift of about +0.7 ppm with regard to the free ligand (Figure 2), and 142.76–146.04 ppm in their ^{1}H and ^{13}C{^{1}H} NMR spectra, respectively, for the NCHN signals (Table 1).

2.2 | Biology

Silver complexes **2a–h** were tested as antimicrobial agents against Gram-negative (*Escherichia coli*, *Pseudomonas aeruginosa*, *Klebsiella pneumoniae*, and *Acinetobacter baumannii*), Gram-positive (*Staphylococcus aureus*, *Staphylococcus aureus* MRSA, and *Enterococcus faecalis*) and fungal (*Candida albicans* and *Candida glabrata*) strains, which were obtained from the American Type Culture Collection (ATCC). The antimicrobial activities of complexes **2a–h** were defined by their minimum inhibitory concentrations (MIC) values, which were defined as the lowest concentration of the antimicrobial that visibly inhibits the growth of microbes after incubation overnight. Ampicillin, amikacin, Ciprofloxacin, fluconazole, vancomycin, and tigecycline served as positive controls in all antimicrobial and antifungal experiments.

As shown in Table 2, the tested complexes displayed antimicrobial activity at certain concentrations from 0.011 to 0.206 μmol/mL. The eight complexes displayed higher activity against fungi with MIC values between 0.011 and 0.026 μmol/mL than against Gram-positive

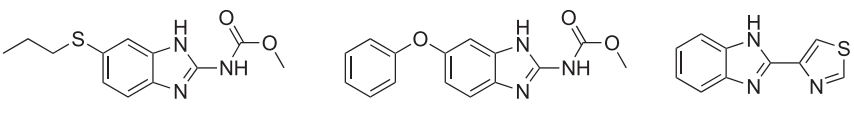
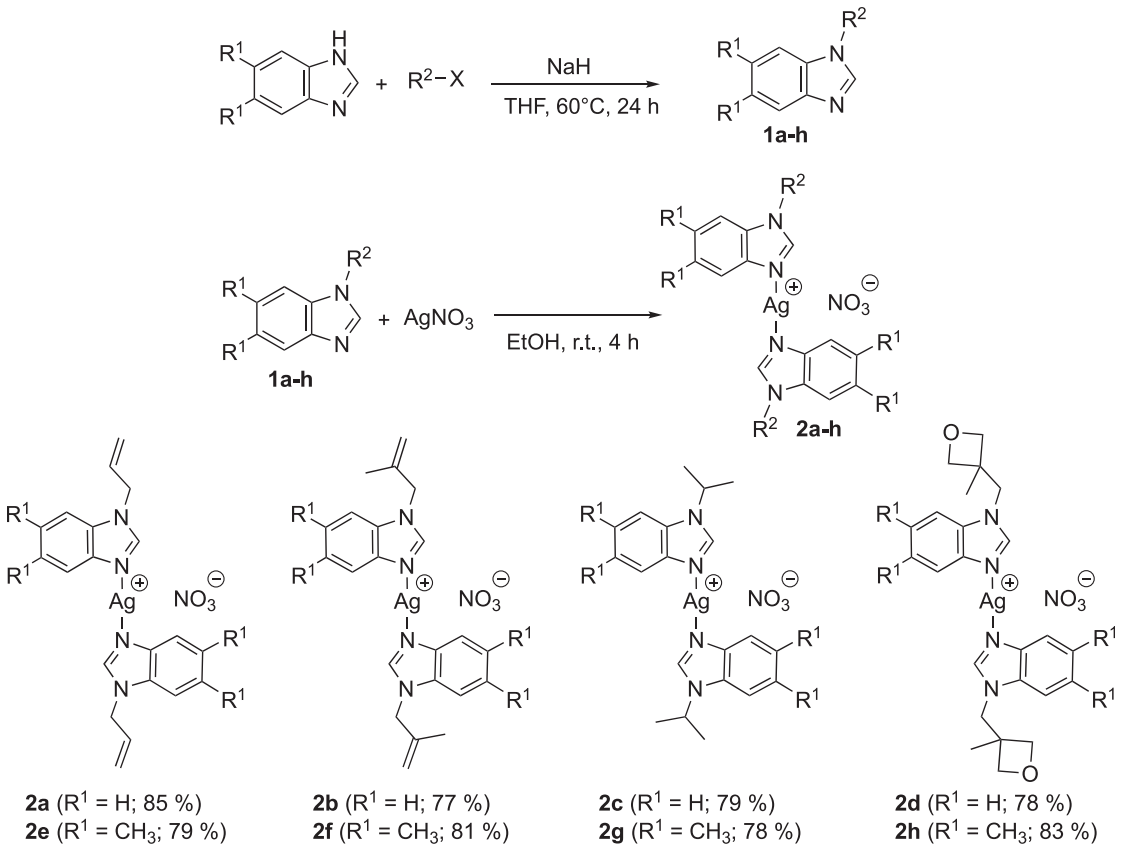


FIGURE 1 Example of commercially available drugs based on benzimidazole skeleton.

15214184, 2023, 10, Downloaded from https://onlinelibrary.wiley.com/doi/10.1002/ardp.202300302 by T C Inonu University , Wiley Online Library on [18/05/2026]. See the Terms and Conditions (https://onlinelibrary.wiley.com/terms-and-conditions) on Wiley Online Library for rules of use; OA articles are governed by the applicable Creative Commons License



SCHEME 1 Synthesis of the bis-*N*-coordinated silver(I) complexes **2a–h**.

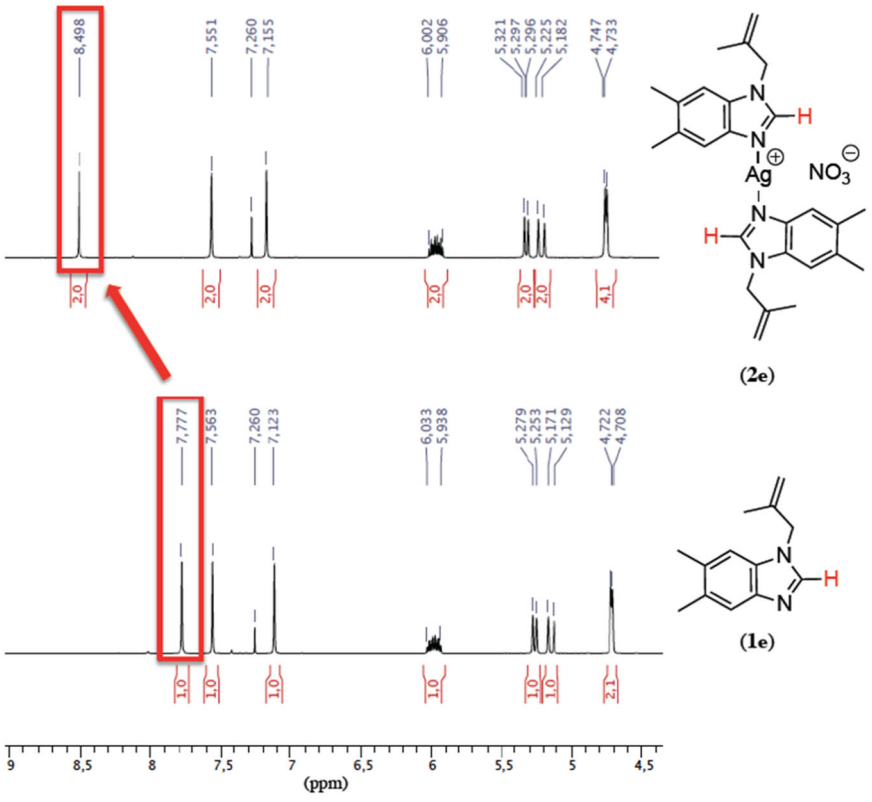


FIGURE 2 ^{1}H NMR spectra of 5,6-dimethyl-benzimidazole **1e** (bottom) and its corresponding silver complex **2e** (top).

15214184, 2023, 10, Downloaded from https://onlinelibrary.wiley.com/doi/10.1002/ardp.202300302 by T C Inonu University , Wiley Online Library on [18/05/2026]. See the Terms and Conditions (https://onlinelibrary.wiley.com/terms-and-conditions) on Wiley Online Library for rules of use; OA articles are governed by the applicable Creative Commons License

and Gram-negative bacteria strains. Although these activities are lower than classical drugs, we can observe that the MIC values measured for the silver complexes **2a–h** are highly dependent on the nature of the alkyl benzimidazole substituent. In addition, the substitutes on the aromatic ring play a crucial role and a match between them is necessary to obtain the strongest antibacterial activities. Thereby, the association of (3-methyloxetan-3-yl)methyl with benzimidazole (complex **2d**) or isopropyl with 5,6-dimethyl-benzimidazole (complex **2g**) led to the lower MIC values (0.087 and 0.091 μmol/mL, respectively) against both Gram-positive and Gram-negative bacteria strains. Additionally, these latter complexes displayed lower MIC values of 0.011 μmol/mL, twice lower than those measured for the standard Fluconazole drug, against *Candida albicans* and *Candida glabrata*.

TABLE 1 Spectroscopic data of silver complexes **2a-h**.

	FT-IR (cm^{-1})		NMR (ppm)	
Silver complex	$\nu(NO_3)$	ν(CN)	^{1}H (NC*H*C)	^{13}C (NCHC)
2a	1329	1507	8.63	145.94
2b	1328	1503	8.68	146.04
2c	1320	1507	8.77	143.45
2d	1331	1511	8.73	145.96
2e	1328	1511	8.50	144.98
2f	1331	1507	8.55	145.20
2g	1316	1515	8.63	142.76
2h	1335	1515	8.59	145.01

2.3 | Molecular docking

In the aim to obtain useful pictures of the interactions of our silver complexes **2a–h** with bacteria and fungal strains, molecular docking[30] was carried out on the crystal structure of *Escherichia coli* deoxyribonucleic acid (DNA) gyrase (PDB ID: 1kzn)[31] and CYP51 from the pathogen *Candida glabrata* (PDB ID: 5jlc) (Table 3).[32]

Escherichia coli DNA gyrase is a bacterial protein of the topoisomerase II family involved in the replication and transcription of DNA and more particularly in the catalysis of the negative supercoiling of closed-circular DNA. Since this function is crucial for DNA replication and transcription, this gyrase has become a target for antibacterial agents. Molecular docking analyses of the silver complexes **2a–h** carried out with *Escherichia coli* DNA gyrase revealed that binding energies values in the range −6.99 to −8.53 kcal/mol, values close to those observed by the group of Soni with phenyl substituted 3-chloro 2-azetidinones.[33] The lowest binding constant was calculated for the **2b** complex, for which a concentration of inhibition of 7.48 μM was determined, and the strongest interactions with the protein involved Ala96 (H-bond), Ile78, Ile90, Asn46 (π-interactions), Val43, Ala47, Val71, Val120, and Val167 (alkyl interactions). As an attempt in view of antibacterial results, the highest binding energies were obtained for **2d** and **2g** with values of −8.53 and −8.28 kcal/mol, respectively with concentrations of inhibition calculated of 557 and 853 nM, respectively. The most important interactions between the complexes **2d** and **2g** and the gyrase were due to Val43, Asp73, Ile90, His95, Thr165 (H-bonds), Asn46, Glu50 (π-interactions), Ile78,

TABLE 2 Minimal inhibitory concentrations (μmol/mL).

	Gram-negative				Gram-positive			Fungi	
Compound	*Escherichia coli*	*Pseudomonas aeruginosa*	*Acinetobacter baumannii*	*Klebsiella pneumoniae*	*Staphylococcus aureus*	*Staphylococcus aureus* MRSA	*Enterococcus faecalis*	*Candida albicans*	*Candida glabrata*
2a	0.103	0.103	0.206	0.103	0.206	0.206	0.206	0.013	0.026
2b	0.097	0.097	0.194	0.097	0.194	0.194	0.194	0.012	0.024
2c	0.204	0.204	0.204	0.204	0.102	0.102	0.102	0.025	0.025
2d	0.087	0.087	0.087	0.087	0.087	0.087	0.087	0.011	0.022
2e	0.184	0.184	0.184	0.184	0.092	0.092	0.092	0.023	0.023
2f	0.175	0.175	0.175	0.175	0.175	0.175	0.175	0.022	0.022
2g	0.091	0.091	0.091	0.091	0.183	0.183	0.183	0.011	0.011
2h	0.159	0.159	0.159	0.159	0.159	0.159	0.159	0.020	0.020
Ampicillin	0.009	/	/	0.004	0.004	/	0.004	/	/
Amikacin	/	0.003	0.005	0.003	/	/	/	/	/
Ciprofloxacin	0.005	/	/	0.005	/	/	/	/	/
Fluconazole	/	/	/	/	/	/	/	0.020	0.020
Vancomycin	/	/	/	/	/	0.002	/	/	/
Tigecycline	/	/	0.003	/	/	/	/	/	/

Note: MRSA, methicillin-resistant *Staphylococcus aureus*.

15214184, 2023, 10, Downloaded from https://onlinelibrary.wiley.com/doi/10.1002/ardp.202300302 by T C Inonu University , Wiley Online Library on [18/05/2026]. See the Terms and Conditions (https://onlinelibrary.wiley.com/terms-and-conditions) on Wiley Online Library for rules of use; OA articles are governed by the applicable Creative Commons License

TABLE 3 Active sites of the crystal structure of *Escherichia coli* DNA gyrase and CYP51 from the pathogen *Candida glabrata* with silver complexes.

Silver complex	Binding energy (kcal/mol)	Amino acid residues
Escherichia coli DNA gyrase (1kzn)		
2a	−7.10	Ile78, Ile90, Ala47, Val71, Val120, Val43, Asn46, Glu50, Gln72, Asp73, Met91...
2b	−6.99	Ala96, Ile78, Ile90, Asn46, Val43, Ala47, Val71, Val120, Val167, Glu50, Gln72...
2c	−7.41	Thr165, Asn46, Ile90, Val43, Ala47, Val71, Ile78, Ala96, Val120, Val167, Glu50...
2d	−8.53	Val43, Asp73, Ile90, His95, Thr165, Asn46, Glu50, Ile78, Val120, Val167, Val71...
2e	−7.97	Thr165, Ile90, Ala47, Val71, Ile78, Val120, Val43, Asn46, Glu50, Gln72, Asp73...
2f	−7.95	Thr165, Asn46, Ile78, Ile90, Val43, Ala47, Val71, Val720, Glu50, Gln72, Asp73...
2g	−8.28	Thr165, Asn46, Ile90, Val43, Ala47, Val71, Ile78, Ala96, Val120, Val167, Glu50...
2h	−8.08	Asp73, Gly77, Ile78, Ile90, Val43, Ala47, Val120, Asn46, Glu50, Val71, Gln72...
CYP51 from the pathogen *Candida glabrata* (5jlc)		
2a	−8.04	Thr319, Ala209, Leu213, Val312, Leu375, Pro380, Leu381, Phe465, Cys472, Ile473...
2b	−8.35	Thr319, Phe465, Val312, Leu375, Pro380, Leu381, Cys472, Ile473, Leu482, Val155...
2c	−8.27	Thr319, Phe465, Leu159, Leu213, Val312, Leu375, His379, Pro380, Leu381, Cys472...
2d	−8.63	Val312, Arg386, His470, Leu381, Phe465, Cys472, Leu159, Leu213, Ile473, Phe477...
2e	−9.01	Thr319, Phe465, Arg471, Ala478, Phe114, Lys152, Leu375, His379, Leu384, Phe477...
2f	−9.38	Gly315, Gly316, Thr319, Arg471, Phe114, Leu148, Lys152, Leu375, His379, Pro380...
2g	−9.25	Thr319, Phe465, Arg471, Ala478, Phe114, Leu375, His379, Pro380, Leu384, Cys472...
2h	−10.14	Thr319, Arg386, Lys152, Arg471, Tyr127, Tyr141, Leu148, Val312, Pro380, His470...

Note: blue, H-bond; red, π-interaction; purple, alkyl interaction; green, van der Waals interaction.

Val120, Val167 (alkyl interactions), and Thr165 (H-bond), Asn46, Ile90 (π-interactions), Val43, Ala47, Val71, Ile78, Ala96, Val120, Val167 (alkyl interactions), respectively (Table 3 and Figure 3). The interaction between these residues and a family of pyrazolyl-imidazole-triazole derivatives as pro-drugs was also highlighted by the group of Verma and confirmed the active region of the target gyrase.[34]

Lanosterol 14 alpha-demethylase is a key enzyme in the ergosterol biosynthesis of fungi as its removal inhibits fungal growth. Azole derivatives are frequently used to provide effective prophylaxis and treatment against superficial and disseminated fungi by coordination with the iron atom in the heme group and therefore inhibiting the latter enzyme.[32,35]

Molecular docking interactions between the silver complexes **2a–h** and the CYP51 crystal structure revealed that the eight complexes interacted with approximately the same region of the target molecule. The highest binding energy, −10.14 kcal/mol, was determined for complex **2h** and was mainly due to H-bonds with Thr319 and Arg389 and π-interaction with Arg471 and Lys152. On the other hand, complex **2a** displayed the lowest interaction value with the target molecule (−8.04 kcal/mol), only one H-bond with Thr319 was calculated, and no π-interaction was detected. No interaction with the iron atom in the heme group was detected. Additionally, inhibition concentrations for complexes **2a–h** were calculated and were in the range of 37 (**2 h**) to 1280 (**2a**) nM (Table 3 and Figure 4).

Structure–activity relationship studies were realized and the highest occupied molecular orbitals (HOMOs) and the lowest unoccupied molecular orbitals (LUMOs), which are approved as the most reactive regions of the molecules, were calculated for complexes **2a–h**. Determination of HOMO and LUMO orbitals gives useful information about the chemical and biological activities of the drugs.[36,37] The HOMO region generally behaves like a Lewis acid, while the LUMO region acts as a Lewis base.[38] In this present study, LUMOs and HOMOs of the eight silver complexes **2a–h** were located on the benzimidazole ring, except for **2d** and **2h**, which, due to the methyloxethane moieties, modified the HOMOs (Figure 5). For each silver complex, the HOMO–LUMO energy gap (Δ*E*), ionization potential, electron affinity, electronegativity, chemical hardness (*η*), and global softness were calculated from the energies of frontier HOMO and LUMO and were reported in Table 4. The latter parameters are important for getting insight into their structure–activity relationships.[39,40] Theoretical calculations have shown that for the eight silver complexes, the gap between HOMO and LUMO varies in the order **2d** (3.188 eV) < **2h** (3.293 eV) < **2f** (3.738 eV) < **2e** (3.741 eV) < **2g** (3.766 eV) < **2a** (3.967 eV) < **2b** = **2c** (3.971 eV). Additionally, the global softness of the complexes **2a–h** follows the same order with a value of 0.314 eV for **2d**. It is well

15214184, 2023, 10, Downloaded from https://onlinelibrary.wiley.com/doi/10.1002/ardp.202300302 by T C Inonu University , Wiley Online Library on [18/05/2026]. See the Terms and Conditions (https://onlinelibrary.wiley.com/terms-and-conditions) on Wiley Online Library for rules of use; OA articles are governed by the applicable Creative Commons License

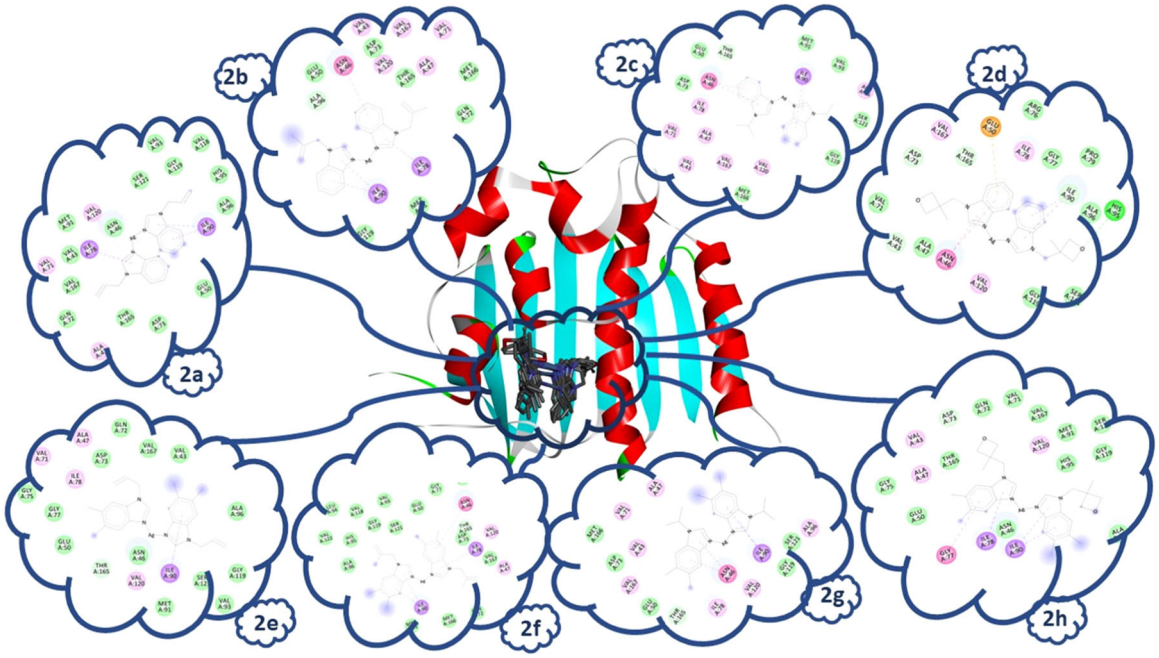


FIGURE 3 Interaction residue (middle), and interaction type of silver complexes **2a–h** with *Escherichia coli* DNA gyrase crystal structure 1kzn (dark green and turquoise: H-bonds; green: van der Waals; orange: pi-anion/cation; pink: alkyl and π-alkyl; yellow: π-sulfur; fuchsia: π–π stacked and π–π T shaped).

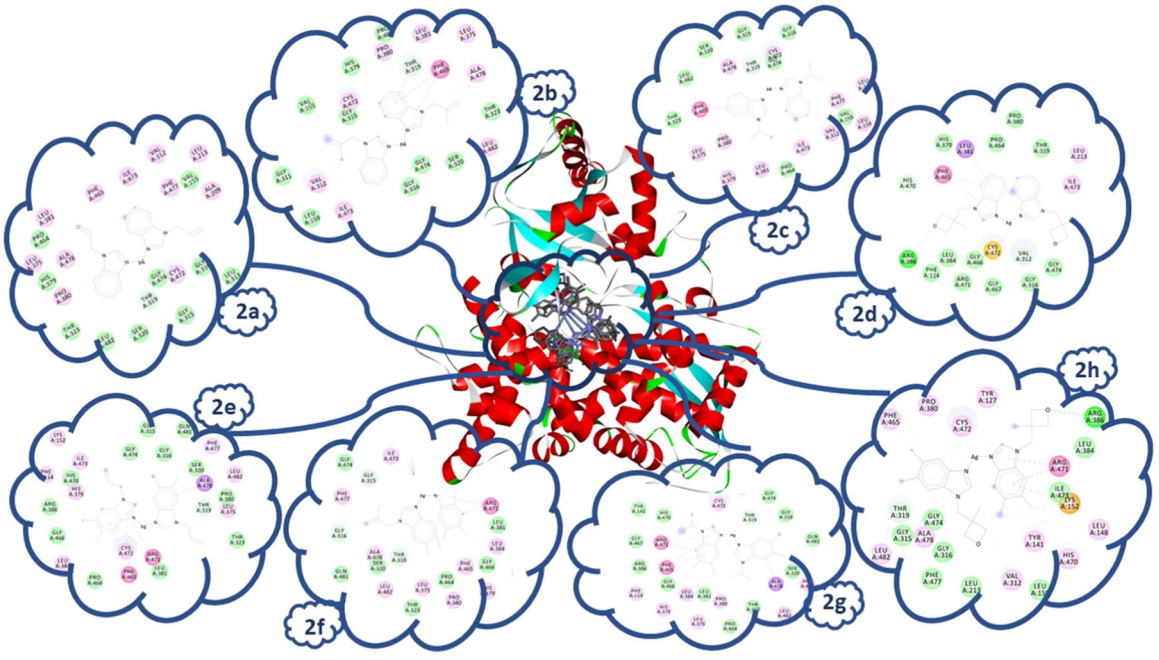


FIGURE 4 Interaction residue (middle), and interaction type of silver complexes **2a–h** with CYP51 from the pathogen *Candida glabrata* crystal structure 5jlc (dark green and turquoise, H-bonds; green, van der Waals; orange, pi-anion/cation; pink, alkyl and π-alkyl; yellow, π-sulfur; fuchsia, π–π stacked and π–π T shaped).

established that the compound with the lowest HOMO–LUMO gap is considered, due to lower kinetic stability and higher polarity, to be softer and more reactive.[41] Therefore, the complex **2d** with the highest softness, the lowest HOMO–LUMO gap, and the lowest chemical hardness should be considered the most reactive molecule. It is interesting to note that these results are corroborated by antimicrobial tests for which complex **2d** displayed the lower MIC values.

15214184, 2023, 10, Downloaded from https://onlinelibrary.wiley.com/doi/10.1002/ardp.202300302 by T C Inonu University , Wiley Online Library on [18/05/2026]. See the Terms and Conditions (https://onlinelibrary.wiley.com/terms-and-conditions) on Wiley Online Library for rules of use; OA articles are governed by the applicable Creative Commons License

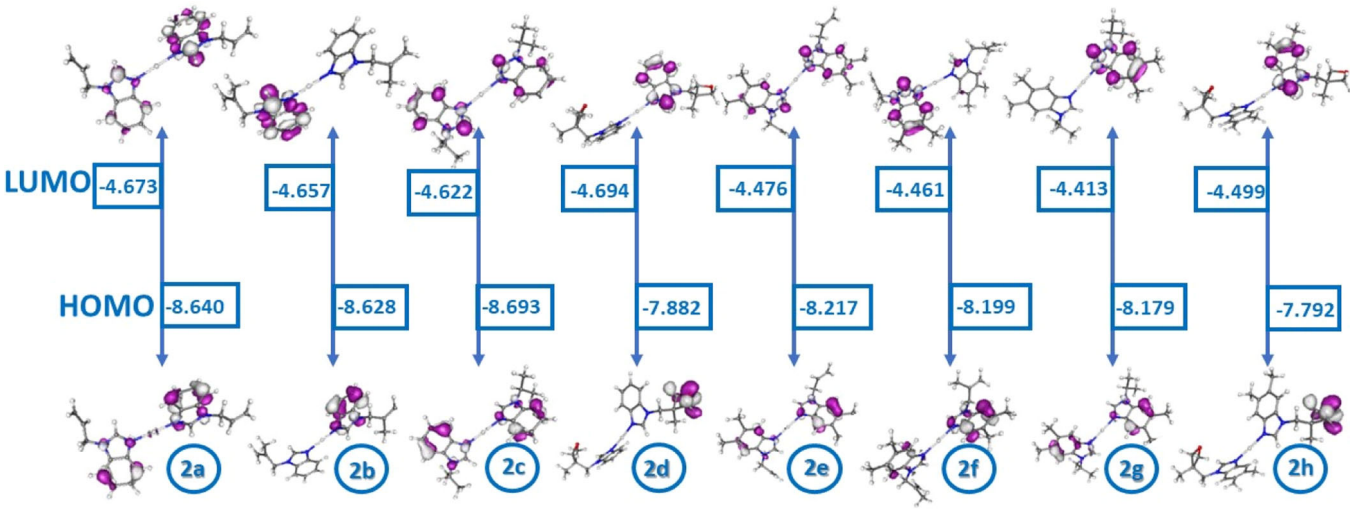


FIGURE 5 Graphical illustrations and the energies of the HOMO and LUMO of silver complexes **2a–h**.

TABLE 4 Global reactivity descriptors of the complexes (in eV).

	2a	2b	2c	2d	2e	2f	2g	2h
HOMO–LUMO gap (Δ*E*)	3.967	3.971	3.971	3.188	3.741	3.738	3.766	3.293
Ionization potential (IP)	8.640	8.628	8.593	7.882	8.217	8.199	8.179	7.792
Electron affinity (EA)	4.673	4.657	4.622	4.694	4.476	4.461	4.413	4.499
Electronegativity (χ)	6.657	6.642	6.607	6.288	6.347	6.330	6.296	6.146
Chemical hardness (η)	1.983	1.985	1.986	1.594	1.870	1.869	1.883	1.647
Global softness (S)	0.252	0.252	0.252	0.314	0.267	0.267	0.265	0.304
Electrophilicity Index (ω)	11.172	11.112	10.993	12.404	10.769	10.719	10.526	11.467

Abbreviations: HOMO, highest occupied molecular orbital; LUMO, lowest unoccupied molecular orbital.

3 | CONCLUSION

Eight silver(I) complexes, in which two 1-alkyl-benzimidazole or 1-alkyl-5,6-dimethyl-benzimidazole were coordinated the metal, were synthetized and fully characterized by FT-IR, elemental analysis, ^{1}H and ^{13}C{^{1}H} NMR spectroscopy. The *N*-coordinated complexes were displayed moderate minimal inhibitory concentrations (MIC) of 0.087 µmol/mL for both Gram-negative and Gram-positive bacteria. The most significant results, with MIC as low as 0.011 µmol/mL and twice lower than those obtained with the commercially available drug flucanozol, were obtained with the *Candida albicans* fungus strain. Additionally, molecular docking on the crystal structures of *Escherichia coli* DNA gyrase and CYP51 from the pathogen *Candida glabrata* revealed that the higher binding energies (up to −10.14 kcal/mol) were calculated for the silver complexes and CYP51. Further studies aim at optimizing the benzimidazole ligand of silver complex to enhance its interactions with the protein CYP51.

4 | EXPERIMENTAL

4.1 | Chemistry

4.1.1 | General

Melting points were recorded in glass capillaries under air with an Electrothermal-9200 melting point apparatus, melting points are reported as uncorrected values. FT-IR spectra were recorded with Perkin Elmer 100 spectrometer. Elemental analyses were done by İnönü University Scientific and Technology Center. ^{1}H and ^{13}C{^{1}H} NMR spectra were recorded with a Bruker Avance III 400 MHz NMR spectrometer. ^{1}H NMR and ^{13}C{^{1}H} NMR spectra were referenced to residual protonated solvents (δ = 7.26 ppm and 77.16 ppm for $CDCl_3$ with tetramethylsilane, respectively, and 2.50 ppm and 39.52 ppm for $(CD_3)_2SO$, respectively). 1-Allyl-benzimidazole (**1a**),[24] 1-(2-methylallyl)-benzimidazole (**1b**),[24] 1-isopropyl-benzimidazole (**1c**),[25] 1-(3-methyloxetan-3-yl)methyl-

15214184, 2023, 10, Downloaded from https://onlinelibrary.wiley.com/doi/10.1002/ardp.202300302 by T C Inonu University , Wiley Online Library on [18/05/2026]. See the Terms and Conditions (https://onlinelibrary.wiley.com/terms-and-conditions) on Wiley Online Library for rules of use; OA articles are governed by the applicable Creative Commons License

benzimidazole (**1d**),[26] 1-allyl-5,6-dimethyl-benzimidazole (**1e**),[27] 1-(2-methylallyl)-5,6-dimethyl-benzimidazole (**1f**)[28] and 1-(3-methyloxetan-3-yl)methyl-5,6-dimethyl-benzimidazole (**1h**)[26] were prepared by literature procedures.

The InChI codes of the investigated compounds, together with some biological activity data, are provided as Supporting Information.

4.1.2 | Procedure for the synthesis of 1-isopropyl-5,6-dimethyl-benzimidazole (**1g**)

The 5,6-dimethyl-benzimidazole (10 mmol) dissolved in dry THF (30 mL) was deprotonated with NaH (10 mmol). The reaction mixture was then stirred for 1 h at room temperature before the dropwise addition of isopropyl chloride (10.1 mmol). The reaction was the heated at 60°C. After 24 h, the THF was removed and the resulted solid was dissolved in dichloromethane (50 mL). The mixture was filtered and the obtained clear solution was concentrated under vacuum to afford compound 1 g in 77% yield. FT-IR: ν(CN) 1471 cm^{-1}; ^{1}H NMR (400 MHz, $CDCl_3$): δ = 1.59 (d, 6H, NCH(CH_3)$_2$, $^3J_{HH}$ = 6.8 Hz), 2.36 (s, 3H, $NC_6H_2N(CH_3)_2$), 2.40 (s, 3H, $NC_6H_2N(CH_3)_2$), 4.56 (hept., 1H, NC*H*(CH_3)$_2$, $^3J_{HH}$ = 6.8 Hz), 7.19 (s, 1H, CH arom), 7.56 (s, 1H, CH arom), 7.88 (s, 1H, NC*H*N): ^{13}C{^{1}H} NMR (100 MHz, $CDCl_3$): δ = 20.27, (s, $NC_6H_2N(CH_3)_2$), 20.59 (s, $NC_6H_2N(CH_3)_2$), 22.64 (s, NCH(CH_3)$_2$), 47.65 (s, NCH(CH_3)$_2$), 110.38, 120.35, 130.94, 131.76, 131.85, 142.66 (6 s, arom Cs), 139.50 (s, NCHN) ppm.

4.1.3 | General procedure for the synthesis of silver(I) complexes **2a–h**

The complexes were synthesized according to the reported procedure.[21] In a Schlenk tube under argon, $AgNO_3$ (0.05 mmol) was added to a stirring solution of benzimidazole (0.10 mmol) in ethanol at room temperature in the dark (wrapped in aluminum foil). After 4 h, the formed precipitate was filtered, washed with diethyl ether (3 × 10 mL) and dried under vacuum to give complexes **2a–h**.

*Bis(1-allyl-benzimidazole)silver(I) nitrate (**2a**)*

Yield: 85%; m.p.: 136–137°C; FT-IR: ν(NO_3) 1329 and ν(CN) 1507 cm^{-1}; ^{1}H NMR (400 MHz, $CDCl_3$): δ = 4.66 (d, 4H, NC*H*$_2$, $^3J_{HH}$ = 6.0 Hz), 5.19 (d, 2H, NCH_2CHCH_2, $^3J_{HH}$ = 17.2 Hz), 5.29 (d, 2H, NCH_2CHCH_2, $^3J_{HH}$ = 10.4 Hz), 5.85–5.95 (m, 2H, NCH_2CHCH_2), 7.31–7.39 (m, 6H, CH arom), 7.82 (d, 2H, arom CH, $^3J_{HH}$ = 8.0 Hz), 8.63 (s, 2H, NC*H*N); ^{13}C{^{1}H} NMR (100 MHz, $CDCl_3$): δ = 48.22 (s, NCH_2), 119.75 (s, NCH_2CHCH_2), 132.57 (s, NCH_2CHCH_2), 110.85, 119.49, 123.83, 124.18, 132.57, 141.46 (6 s, arom Cs), 145.94 (s, NCHN) ppm. Elemental analysis (%): calcd for $C_{20}H_{20}AgN_5O_3$ (486.28): C: 49.40; H: 4.15; N: 14.40; found C: 49.33; H: 3.89; N: 14.42.

*Bis[1-(2-methylallyl)-benzimidazole]silver(I) nitrate (**2b**)*

Yield: 77%; m.p.: 130–131°C; FT-IR: ν(NO_3) 1328 and ν(CN) 1503 cm^{-1}; ^{1}H NMR (400 MHz, $(CD_3)_2SO$): δ = 1.68 (s, 6H, $NCH_2C(CH_3)CH_2$), 4.75 (s, 2H, $NCH_2C(CH_3)CH_2$), 4.97 (s, 2H, $NCH_2C(CH_3)CH_2$), 5.02 (s, 4H, NCH_2), 7.36-7.41 (m, 4H, CH arom), 7.67–7.70 (m, 2H, CH arom), 7.88-7.80 (m, 2H, CH arom), 8.68 (s, 2H, NC*H*N); ^{13}C{^{1}H} NMR (100 MHz, $(CD_3)_2SO$): δ = 19.58 (s, $NCH_2C(CH_3)CH_2$), 50.40 (s, NCH_2), 113.06 (s, $NCH_2C(CH_3)CH_2$), 140.24 (s, $NCH_2C(CH_3)CH_2$), 111.66, 119.27, 123.14, 123.83, 132.91, 141.39 (6 s, arom Cs), 146.04 (s, NCHN) ppm. Elemental analysis (%): calcd for $C_{22}H_{24}AgN_5O_3 \bullet H_2O$ (532.35): C: 49.64; H: 4.92; N: 13.16; found C: 49.39; H: 4.34; N: 13.85.

*Bis(1-isopropyl-benzimidazole)silver(I) nitrate (**2c**)*

Yield: 79%; m.p.: 132–133°C; FT-IR: ν(NO_3) 1320 and ν(CN) 1507 cm^{-1}; ^{1}H NMR (400 MHz, $(CD_3)_2SO$): δ = 1.60 (d, 12H, NCH(CH_3)$_2$, $^3J_{HH}$ = 6.8 Hz), 4.92 (hept, 2H, NC*H*(CH_3)$_2$, $^3J_{HH}$ = 6.8 Hz), 7.36–7.43 (m, 4H, CH arom), 7.82–7.85 (m, 2H, CH arom), 7.90–7.92 (m, 2H, CH arom), 8.77 (s, 2H, NC*H*N); ^{13}C{^{1}H} NMR (100 MHz, $(CD_3)_2SO$): δ = 22.08 (s, NCH(CH_3)$_2$), 48.17 (s, NCH(CH_3)$_2$), 111.79, 119.32, 123.14, 123.66, 132.06, 141.53 (6 s, arom Cs), 143.45 (s, NCHN) ppm. Elemental analysis (%): calcd for $C_{20}H_{24}AgN_5O_3 \bullet H_2O$ (508.33): C: 47.26; H: 5.15; N: 13.78; found C: 47.53; H: 4.75; N: 14.12.

*Bis(1-(3-methyloxetan-3-yl)methyl-benzimidazole)silver(I) nitrate (**2d**)*

Yield: 76%; m.p.: 160–161°C; FT-IR: ν(NO_3) 1331 and ν(CN) 1511 cm^{-1}; ^{1}H NMR (400 MHz, $(CD_3)_2SO$): δ = 1.26 (s, 6H, NCH_2CCH_3), 4.26 and 4.59 (AB spin system, 8H, CCH_2O, $^2J_{HH}$ = 6.0 Hz), 4.63 (s, 4H, NCH_2), 7.36–7.44 (m, 4H, CH arom), 7.84–7.89 (m, 4H, CH arom), 8.73 (s, 2H, NC*H*N); ^{13}C{^{1}H} NMR (100 MHz, $(CD_3)_2SO$): δ = 21.86 (s, NCH_2CCH_3), 40.68 (s, NCH_2CCH_3), 50.30 (s, NCH_2CCH_3), 78.92 (s, CCH_2O), 111.65, 119.25, 123.60, 123.92, 133.72, 141.02 (6 s, arom Cs), 145.96 (s, NCHN) ppm. Elemental analysis (%): calcd for $C_{24}H_{28}AgN_5O_5 \bullet H_2O$ (592.40): C: 48.66; H: 5.10; N: 11.82; found C: 47.01; H: 4.60; N: 11.44.

*Bis(1-allyl-5,6-dimethyl-benzimidazole)silver(I) nitrate (**2e**)*

Yield: 79%; m.p.: 156–157°C; FT-IR: ν(NO_3) 1328 and ν(CN) 1511 cm^{-1}; ^{1}H NMR (400 MHz, $CDCl_3$): δ = 2.38 (brs, 12H, $C_6H_2(CH_3)_2$), 4.74 (d, 4H, NCH_2, $^3J_{HH}$ = 5.6 Hz), 5.20 (d, 2H, NCH_2CHCH_2, $^3J_{HH}$ = 17.2 Hz), 5.30 (d, 2H, NCH_2CHCH_2, $^3J_{HH}$ = 10.0 Hz), 5.91–6.00 (m, 2H, NCH_2CHCH_2), 7.15 (s, 2H, CH arom), 7.55 (s, 2H, arom CH), 8.50 (s, 2H, NC*H*N); ^{13}C{^{1}H} NMR (100 MHz, $CDCl_3$): δ = 20.43 (s, $C_6H_2(CH_3)_2$), 20.69 (s, $C_6H_2(CH_3)_2$), 48.18 (s, NCH_2), 119.33 (s, NCH_2CHCH_2), 131.25 (s, NCH_2CHCH_2), 110.97, 119.45, 131.29, 133.09, 133.80, 140.27 (6 s, arom Cs), 144.98 (s, NCHN) ppm. Elemental analysis (%): calcd for $C_{24}H_{28}AgN_5O_3$ (542.39): 53.15; H: 5.20; N: 12.91; found C: C: 53.60; H: 5.19; N: 12.90.

*Bis[1-(2-methylallyl)-5,6-dimethyl-benzimidazole]silver(I) nitrate (**2f**)*

Yield: 81%; m.p.: 171–172°C; FT-IR: ν(NO_3) 1331 and ν(CN) 1507 cm^{-1}; ^{1}H NMR (400 MHz, $(CD_3)_2SO$): δ = 1.68 (s, 6H, $NCH_2C(CH_3)CH_2$), 2.33 (s, 6H, $C_6H_2(CH_3)_2$), 2.35 (s, 6H, $C_6H_2(CH_3)_2$), 4.70 (s, 2H, $NCH_2C(CH_3)CH_2$), 4.95 (brs, 6H, $NCH_2C(CH_3)CH_2$ and NCH_2), 7.45 (s, 2H, CH arom), 7.66 (s, 2H, CH arom), 8.55 (s, 2H, NC*H*N); ^{13}C{^{1}H} NMR (100 MHz, $(CD_3)_2SO$): δ = 19.61 (s, $NCH_2C(CH_3)CH_2$), 19.91 (s, $NCH_2C(CH_3)CH_2$), 19.99

15214184, 2023, 10, Downloaded from https://onlinelibrary.wiley.com/doi/10.1002/ardp.202300302 by T C Inonu University , Wiley Online Library on [18/05/2026]. See the Terms and Conditions (https://onlinelibrary.wiley.com/terms-and-conditions) on Wiley Online Library for rules of use; OA articles are governed by the applicable Creative Commons License

(s, $C_6H_2(CH_3)_2$), 20.16 (s, $C_6H_2(CH_3)_2$), 50.33 (s, NCH_2), 112.80 (s, $NCH_2C(CH_3)CH_2$), 140.34 (s, $NCH_2C(CH_3)CH_2$), 111.48, 119.03, 131.39, 132.02, 132.95, 139.84 (6 s, arom Cs), 145.20 (s, NCHN) ppm. Elemental analysis (%): calcd for $C_{26}H_{32}AgN_5O_3$ (570.44): C: 54.74; H: 5.65; N: 12.28; found C: 55.98; H: 5.26; N: 12.66.

*Bis(1-isopropyl-5,6-dimethyl-benzimidazole)silver(I) nitrate (**2g**)*

Yield: 78%; m.p.: 205–206°C; FT-IR: $\nu(NO_3)$ 1316 and ν(CN) 1515 cm^{-1}; ^{1}H NMR (400 MHz, $CDCl_3$): δ = 1.65 (d, 12H, NCH(CH_3)$_2$, $^3J_{HH}$ = 6.4 Hz), 2.41 (s, 6H, $C_6H_2(CH_3)_2$), 2.42 (s, 6H, $C_6H_2(CH_3)_2$), 4.64 (hept, 2H, NC*H*$(CH_3)_2$, $^3J_{HH}$ = 6.4 Hz), 7.27 (s, 2H, CH arom), 7.55 (s, 2H, CH arom), 8.63 (s, 2H, NC*H*N); ^{13}C{^{1}H} NMR (100 MHz, $CDCl_3$): δ = 20.44 (s, $C_6H_2(CH_3)_2$), 20.76 (s, $C_6H_2(CH_3)_2$), 22.49 (s, NCH$(CH_3)_2$), 48.97 (s, NCH$(CH_3)_2$), 111.27, 119.33, 130.79, 132.93, 133.44, 140.58 (6 s, arom Cs), 142.76 (s, NCHN) ppm. Elemental analysis (%): calcd for $C_{24}H_{32}AgN_5O_3 \bullet H_2O$ (564.43): C: 51.07; H: 6.07; N: 12.41; found C: 50.75; H: 6.77; N: 13.24.

*Bis(1-(3-methyloxetan-3-yl)methyl-5,6-dimethyl-benzimidazole) silver(I) nitrate (**2h**)*

Yield: 83%; m.p.: 284–285°C; FT-IR: $\nu(NO_3)$ 1335 and ν(CN) 1515 cm^{-1}; ^{1}H NMR (400 MHz, $(CD_3)_2SO$): δ = 1.25 (s, 6H, NCH_2CCH_3), 2.34 (s, 6H, $C_6H_2(CH_3)_2$), 2.37 (s, 6H, $C_6H_2(CH_3)_2$), 4.25 and 4.53 (AB spin system, 8H, CCH_2O, $^2J_{HH}$ = 6.0 Hz), 4.60 (s, 4H, NCH_2), 7.62 (s, 2H, CH arom), 7.64 (s, 2H, CH arom), 8.59 (s, 2H, NC*H*N); ^{13}C{^{1}H} NMR (100 MHz, $(CD_3)_2SO$): δ = 19.87 (s, $C_6H_2(CH_3)_2$), 20.20 (s, $C_6H_2(CH_3)_2$), 21.87 (s, NCH_2CCH_3), 40.65 (s, NCH_2CCH_3), 50.25 (s, NCH_2CCH_3), 78.93 (s, CCH_2O), 111.45, 119.00, 131.80, 132.24, 133.97, 139.57 (6 s, arom Cs), 145.01 (s, NCHN) ppm. Elemental analysis (%): calcd for $C_{28}H_{36}AgN_5O_5$ (630.49): C: 53.34; H: 5.75; N: 11.11; found C: 53.27; H: 5.66; N: 10.96.

4.2 | Biological assays

The antimicrobial activity assays of silver(I) complexes **2a–h** substances were carried out using the modified agar dilution method recommended by the Clinical and Laboratory Standards Institute (CLSI).[42,43] The MIC values of the compounds were determined using the microwell dilution method for the bacterial and fungal strains (American Type Culture Collection ATCC). Bacterial strains: *Staphylococcus aureus* ATCC 29213, *Enterococcus faecalis* ATCC 29212, *Escherichia coli* ATCC 25922, *Pseudomonas aeruginosa* ATCC 27853, *Staphylococcus aureus* MRSA ATCC 43300, *Klebsiella pneumoniae* ATCC 700603, and *Acinetobacter baumannii* ATCC 19606; mushroom strains: *Candida glabrata* ATCC 90030 and *Candida albicans* ATCC 14053.

Bacterial strains were grown in Muller Hinton Broth (Merck) medium, and fungal strains were grown in RPMI 1640 Broth (Sigma-Aldrich Chemie GmbH Taufkirchen) medium. Turbidity of bacteria and fungi matched that of a McFarland no. 0.5 turbidity standard.[44] The prepared bacterial and fungal standard inoculums were inoculated into the media as two series for control and growth was detected in all of them. Solutions of all compounds were prepared in DMSO. All dilutions were made with distilled water. Concentrations of test compounds are 800, 400, 200, 100, 50, 25, 12.5, and 6.25 µg/mL. The MIC values were further expressed in µmol/mL

Ampicillin, ciprofloxacin, amikacin, tigecycline, and vancomycin were used as antibacterial standard drugs, while fluconazole was used as an antifungal standard drug. Standard inoculum of bacteria and fungi (106 CFUs/mL) were inoculated with a sterile plastic ring-tipped loop (0.01 mL) on agar plates containing 800, 400, 200, 100, 50, 25, 12.5, and 6.25 µg/mL material. All planted plates were evaluated after they were kept in an oven at 35°C for 16–20 h for bacteria and 48 h for fungi. MIC was determined as the lowest concentration preventing bacteria and fungi growth.

4.3 | Molecular docking

ORCA package version 4.0[45,46] was used for geometry optimization with BP86[47,48] functional and with a def2-SVP def2-SVP/J basis set. density functional theory (DFT) calculations were restricted with KDIIS SOSCF and tightscf options. The crystal structures of the target molecules were downloaded from RCSB Protein Data Bank (https://www.rcsb.org/) (PDB ID: 1kzn and 5jlc).[31,32] The molecular docking calculations were performed with AutoDock 4.2.[49,50] Only polar hydrogens were evaluated and Kollman charges were used during the procedures. The water molecules were removed from the targets. The processes were started with randomized positions for silver complex with Gasteiger charges. Lamarckian genetic algorithms were employed with 150 genetic algorithm populations.[51]

4.4 | DFT-based calculation methods

ORCA package version 4.0[45,52] was used for geometry optimization with BP86 functional and with a def2-SVP def2-SVP/J basis set.[47,48] DFT calculations were restricted with KDIIS SOSCF and tightscf options. The chemical reactivity descriptors were calculated with Koopmans Theorem according to following equations.[53,54]

$$\text{Ionization potential: } IP = -E_{HOMO}, \quad (1)$$

$$\text{Electron affinity: } EA = -E_{LUMO}, \quad (2)$$

$$\text{Electronegativity: } \chi = -(I + A)/2, \quad (3)$$

$$\text{Chemical hardness: } \eta = (I - A)/2, \quad (4)$$

$$\text{Global softness: } S = 1/2\eta, \quad (5)$$

$$\text{Electrophilicity index: } \omega = \hat{\mu}/2\eta. \quad (6)$$

ACKNOWLEDGMENTS

This work is supported by the Scientific Research Project Fund of Sivas Cumhuriyet University (project number F-461).

15214184, 2023, 10, Downloaded from https://onlinelibrary.wiley.com/doi/10.1002/ardp.202300302 by T C Inonu University , Wiley Online Library on [18/05/2026]. See the Terms and Conditions (https://onlinelibrary.wiley.com/terms-and-conditions) on Wiley Online Library for rules of use; OA articles are governed by the applicable Creative Commons License

CONFLICTS OF INTEREST STATEMENT

The authors declare no conflicts of interest.

ORCID

Elvan Üstün http://orcid.org/0000-0002-0587-7261
İsmail Özdemir http://orcid.org/0000-0001-6325-0216
David Sémeril http://orcid.org/0000-0002-2582-4191

REFERENCES

[1] M. M. Heravi, V. Zadsirjan, *RSC Adv*. **2020**, *10*, 44247.
[2] Q. A. McKellar, E. W. Scott, *J. Vet. Pharmacol. Ther*. **1990**, *13*, 223.
[3] A. A. Spasov, I. N. Yozhitsa, L. I. Bugaeva, V. A. Anisimova, *Pharm. Chem. J*. **1999**, *33*, 232.
[4] A. Patil, S. Ganguly, S. Surana, *Rasayan J. Chem*. **2008**, *1*, 447.
[5] A. Husain, M. M. Varshney, M. Rashid, R. Mishra, A. Akhter, *J. Pharm. Res*. **2011**, *4*, 413.
[6] Y. Bansal, O. Silakari, *Bioorg. Med. Chem*. **2012**, *20*, 6208.
[7] A. S. Gurkan-Alp, H. Göker, M. Alp, T. Ozkan, A. Sunguroglu, *Arch. Pharmacal Res*. **2015**, *38*, 650.
[8] S. R. Brishty, M. J. Hossain, M. U. Khandaker, M. R. I. Faruque, H. Osman, S. M. A. Rahman, *Front. Pharmacol*. **2021**, *12*, 762807.
[9] D. V. Maltsev, A. A. Spasov, P. M. Vassiliev, M. O. Skripka, M. V. Miroshnikov, A. N. Kochetkov, N. V. Eliseeva, Y. V. Lifanova, T. A. Kuzmenko, L. N. Divaeva, A. S. Morkovnik, *Molecules* **2021**, *26*, 6049.
[10] A. S. Al-Wasidi, M. Refat, A. M. Naglah, A. A. Elhenawy, *Egypt. J. Chem*. **2021**, *64*, 2631.
[11] M. Marinescu, *Antibiotics* **2021**, *10*, 1002.
[12] S. Suerbaum, H. Leying, K. Klemm, W. Opferkuch, *Eur. J. Clin. Microbiol. Infect. Dis*. **1991**, *10*, 92.
[13] H. Rostami, M. H. Haddadi, *Fundam. Clin. Pharmacol*. **2022**, *36*, 930.
[14] H. Hernández-López, C. J. Tejada-Rodríguez, S. Leyva-Ramos, *Mini-Rev. Med. Chem*. **2022**, *22*, 1268.
[15] C. Cray, N. H. Altman, *Comp. Med*. **2022**, *72*, 215.
[16] S. O. Podunavac-Kuzmanovic, D. M. Cvetkovic, *J. Serb. Chem. Soc*. **2007**, *72*, 459.
[17] X. Wang, N. Ling, Q.-T. Che, Y.-W. Zhang, H.-X. Yang, Y. Ruan, T.-T. Zhao, *Inorg. Chem. Commun*. **2019**, *105*, 97.
[18] I. D. Vlaicu, R. Olar, C. Maxim, M. C. Chifiriuc, C. Bleotu, N. Stănică, G. Vasile Scăeţeanu, C. Dulea, S. Avram, M. Badea, *Appl. Organomet. Chem*. **2019**, *33*, e4976.
[19] Z. Šindelář, P. Kopel, *Inorganics* **2023**, *11*, 113.
[20] A. Rauf, J. Ye, A. Hao, L. Zhao, S. Zhang, Y. Qi, L. Shi, G. Ning *J. Coord. Chem. 71*, **2018**, 3266.
[21] M. O. Karataş, N. Özdemir, M. Sarıman, S. Günal, E. Ulukaya, İ. Özdemir, *Dalton Trans*. **2021**, *50*, 11596.
[22] S. Y. Hussaini, R. A. Haque, U. F. M. Haziz, A. A. Amirul, M. R. Razali, *J. Mol. Struct*. **2021**, *1246*, 131187.
[23] R.Y. Nadeem, M. Yaqoob, W. Yam, R. A. Haque, M. A. Iqbal, *Med. Chem. Res*. **2022**, *31*, 1783.
[24] N. Şahin, İ. Yıldırım, N. Özdemir, N. Gürbüz, İ. Özdemir, *J. Organomet. Chem*. **2020**, *918*, 121285.v.
[25] Y.-R. Lin, C.-C. Chiu, H.-T. Chiu, D.-S. Lee, T.-J. Lu, *Appl. Organomet. Chem*. **2017**, *32*, e3896.
[26] Z. Nawaz, N. Gürbüz, M. N. Zafar, N. Özdemir, U. Habib, K. Jan, K. İ. Özdemir, *J. Mol. Struct*. **2021**, *1243*, 130883.
[27] E. Üstün, N. Şahin, C. Çelik, U. Tutar, N. Özdemir, N. Gürbüz, İ. Özdemir, *Dalton Trans*. **2021**, *50*, 15400.
[28] N. Şahin, E. Üstün, U. Tutar, C. Çelik, N. Gürbüz, İ. Özdemir, *J. Organomet. Chem*. **2021**, *954*, 122082.
[29] Ö. Karlık, S. Balcıoğlu, M. O. Karataş, B. Ateş, B. Alıcı, N. Özdemir, *Polyhedron* **2018**, *142*, 63.
[30] D. A. Gschwend, A. C. Good, I. D. Kuntz, *J. Mol. Recognit*. **1996**, *9*, 175.
[31] D. Lafitte, V. Lamour, P. O. Tsvetkov, A. A. Makarov, M. Klich, P. Deprez, D. Moras, C. Briand, R. Gilli, *Biochemistry* **2002**, *41*, 7217.
[32] M. V. Keniya, M. Sabherwal, R. K. Wilson, M. A. Woods, A. A. Sagatova, J. D. A. Tyndall, B. C. Monka, *Antimicrob. Agents Chemother*. **2018**, *62*, e01134.
[33] R. V. Kusurkar, R. H. Rayani, D. R. Parmar, D. R. Patel, M. J. Patel, N. O. Pandey, V. Zunjar, J. Y. Soni, *J. Mol. Struct*. **2023**, *1272*, 134185.
[34] S. Punia, V. Verma, D. Kumar, A. Kumar, L. Deswal, G. Singh, S. C. Sahoo, *J. Mol. Struct*. **2022**, *1262*, 133060.
[35] A. Özdemir, B. Sever, M. D. Altıntop, *Lett. Drug. Des. Discov*. **2019**, *16*, 82.
[36] A. Ö. Kiraz, M. Koca, A. Kurt, İ. Kara, C. Arıcı, *J. Mol. Struct*. **2022**, *1259*, 132702.
[37] A. Fatima, G. Khanum, A. Sharma, N. Siddiqui, S. Muthu, R. J. Butcher, S. K. Srivastava, S. Javed, *J. Mol. Struct*. **2022**, *1268*, 133613.
[38] M. Hara, *Bull. Chem. Soc. Jpn*. **2014**, *87*, 931.
[39] S. Andrade-Ochoa, G. V. Nevárez-Moorillón, L. E. Sánchez-Torres, M. Villanueva-García, B. E. Sánchez-Ramírez, L. M. Rodríguez-Valdez, B. E. Rivera-Chavira, *BMC Complement. Altern. Med*. **2015**, *15*, 332.
[40] S. A. Ejaz, M. Zain-ul-Abideen, P. A. Channar, A. Saeed, A. Ahmed, N. S. Alsaiari, K. M. Katubi, Q. Abbas, K. A. Dahlous, H. Raza, S. J. Kim, M. N. Mustafa, *J. Mol. Struct*. **2023**, *1282*, 135225.
[41] M. M. Hoque, M. A. Halim, M. G. Sarwar, M. W. Khan, *J. Phys. Org. Chem*. **2015**, *28*, 732.
[42] Clinical and Laboratory Standards Institute, *Methods for antimicrobialdilution and disk susceptibility testing of infrequently isolated or fastidious bacteria. Approved standard M45-A*. (Eds: P. A. Wayne), Clinical and Laboratory Standards Institute, **2006**.
[43] Clinical and Laboratory Standards Institute, *Reference method for broth dilution antifungal susceptibility testing of yeasts. Approved standard M27-S4*. (Eds: P. A. Wayne), Clinical and Laboratory Standards Institute, **2012**.
[44] J. Hindler, L. Hochstein, A. Howell, in *Clinical Microbiology Procedures Handbook* (Ed: H. D. Isenberg), American Society for Microbiology, Washington, DC **1992**.
[45] F. Neese, *WIREs Comput. Mol. Sci*. **2012**, *2*, 73.
[46] F. Neese, *WIREs Comput. Mol. Sci*. **2017**, *8*, e1327.
[47] J. P. Perdew, *Phys. Rev. B: Condens. Matter Mater. Phys*. **1986**, *33*, 8822.
[48] A. D. Becke, *Phys. Rev. A*. **1988**, *38*, 3098.
[49] O. Trott, A. J. Olson, *J. Comput. Chem*. **2010**, *31*, 455.
[50] S. Forli, R. Huey, M. E. Pique, M. F. Sanner, D. S. Goodsell, A. J. Olson, *Nat. Protoc*. **2016**, *11*, 905.
[51] G. M. Morris, D. S. Goodsell, R. S. Halliday, R. Huey, W. E. Hart, R. K. Belew, A. J. Olson, *J. Comput. Chem*. **1998**, *19*, 1639.
[52] F. Neese, *WIREs Comput. Mol. Sci*. **2018**, *8*, e1327.
[53] T. Tsuneda, J.-W. Song, S. Suzuki, K. Hirao, *J. Chem. Phys*. **2010**, *133*, 174101.
[54] N. Şahin, M. S. Çelebi, M. Ç. Ayvaz, E. stün, *Inorg. Chem. Commun*. **2022**, *145*, 110028.

SUPPORTING INFORMATION

Additional supporting information can be found online in the Supporting Information section at the end of this article.

How to cite this article: E. Üstün, N. Şahin, İ. Özdemir, S. Günal, N. Gürbüz, İ. Özdemir, D. Sémeril, *Arch. Pharm.* **2023**;*356*:e2300302. https://doi.org/10.1002/ardp.202300302

15214184, 2023, 10, Downloaded from https://onlinelibrary.wiley.com/doi/10.1002/ardp.202300302 by T C Inonu University , Wiley Online Library on [18/05/2026]. See the Terms and Conditions (https://onlinelibrary.wiley.com/terms-and-conditions) on Wiley Online Library for rules of use; OA articles are governed by the applicable Creative Commons License